Article

Generalized Dynamical Modeling of Multiple Photovoltaic Units in a Grid-Connected System for Analyzing Dynamic Interactions

Tahsin Fahima Orchi, Md Apel Mahmud * ⃝ and Amanullah Maung Than Oo

Electrical Power & Energy Systems Research Laboratory (EPESRL), School of Engineering, Deakin University, Geelong, VIC 3216, Australia; torchi@deakin.edu.au (T.F.O.); aman.m@deakin.edu.au (A.M.T.O.)
* Correspondence: apel.mahmud@deakin.edu.au; Tel.: +61-3-5227-1214

Abstract: This paper aims to develop the generalized dynamical model of multiple photovoltaic (PV) units connected to the grid along with the dynamic interaction analysis among different PV units. The dynamical models of multiple PV units are developed by considering three different configurations through which these PV units are connected to the grid. These configurations include: (a) the direct connection of multiple PV units to the grid; (b) the connection of multiple PV units to the grid through a point of common coupling (PCC); and (c) the connection of PV units without a PCC. The proposed modeling framework provides meaningful insights for analyzing dynamic interaction analysis where these interactions from other PV units are expressed in terms of voltages and line impedances rather than the dynamics of currents. The dynamic interactions among different PV units for all these configurations are analyzed using both analytical and simulation studies. Simulations are carried out on an IEEE 15-bus test system and dynamic interactions are analyzed from the total harmonic distortions (THDs) in the current responses of different PV units. Both analytical and simulation studies clearly indicate that the effects of dynamic interactions are prominent with the increase in PV units.

Keywords: dynamical modeling; dynamic interactions; multiple PV units; grid-connected system

1. Introduction

Assessments of renewable energy potential are gaining much interest worldwide due to the inceptions of self-reliant energy generation schemes. Such inceptions promote the utilization of renewable energy sources (RESs) in the form of microgrids [1,2] and also reduce the pressure on conventional fossil fuels which in turn reduce the greenhouse gas emissions [3–5]. According to the National Electricity Forecasting Report, the solar energy is the largely installed RES in Australia in terms of the proportion of houses and it is expected that by 2035–2036, the small-scale photovoltaic (PV) capacity will approximately be 20.1 GW [6]. However, the large number of PV systems raise new technical challenges such as grid interconnections, protections, stability, and power quality issues [3,7]. On the contrary, close proximities of multiple PV systems at the distribution system level may lead to interactions or unwanted oscillations which severely affect the overall operational efficiency of the system [8].

The consequences of connecting multiple PV units with the existing power grid are referred as the deterioration of power quality which is usually measured in terms of total harmonic distortions (THDs) and instability due to the poor damping characteristics of the system [9–11]. Since the output power from the solar PV units is DC power and power conditioning units, i.e., voltage source inverters (VSIs) are used for power conversions, there always exist some harmonics in the output AC power [12]. Moreover, the atmospheric conditions such as the solar irradiation and temperature change

frequently for which the stability of the whole system is affected. The impacts of large penetration of solar PV systems are evaluated in [13,14] using simulation studies under different conditions. Recently, the dynamic voltage stability of grid-connected PV systems are analyzed in [15] due to changes in its load and operating conditions. In [13–15], the analyses are performed based on the available models in the simulation tools. However, the models available in the simulation tools do not provide useful insights to have clear understanding about dynamic characteristics of PV units in grid-connected systems.

The dynamical modeling and simulation of grid-connected PV systems are performed in [16–19] where the model are basically developed for a single PV units though, in some cases, the analyses are conducted by considering large-scale power systems [20,21]. In these literature, the analyses are basically conducted to investigate the dynamic interactions in terms of THD in the injected current by each PV unit as well as to analyze the stability of the whole system [22]. In [23], the dynamic stability of large-scale distributed solar PV systems is analyzed by considering a practical case study while the dynamical models of PV unit are still considered as similar to that of a single PV unit. The small-signal stability analysis of a large distribution system with a number of PV units are analyzed in [24] through eigenvalue analysis while the dynamical models for each PV unit are considered as similar to that in [23]. However, the analyses based on the dynamical model of a single PV unit does not reflect the actual dynamic interactions within the system.

The modeling of *N*-parallel grid-connected inverters for PV applications are presented in [25] by considering *LCL* output filters. In [25], each parallel inverter is directly connected to the grid and the dynamical models are developed for each model which do not reflect any interaction due to the inclusion of multiple PV units. Recently, a similar approach is used in [26] to represent the dynamical models of multiple PV units. However, the problem of solving dynamic interactions based on the dynamical models remains unsolved. The dynamic characteristics of multiple PV units are analyzed in [27] where it is considered that all PV units are connected in a microgrid. However, the dynamical model in [27] does not include the effects of dynamic interactions due to other PV units within the microgrid.

The analysis of dynamic interactions and design of controllers require meaningful dynamical models in order to eliminate the negative impacts of such interactions and maintain the stability of the whole system. The existing literature, so far discussed in this paper, does not provide useful insights regarding the dynamic interactions in a grid-connected system with multiple PV units though there exist some rigorous analytical studies. However, all these analyses depend on the dynamical models and these are significantly affected due to the use of simplified dynamical models. Moreover, the dynamical models also depend on the configurations through which PV units are connected to the grid. For example, PV units may be directly connected to the grid, through a point of common coupling, and through lines. Thus, it is worth to develop generalized dynamical model by considering all possible configurations, analyze dynamic interactions, and design controllers based on such models.

This paper aims to develop generalized dynamical models for grid-connected systems with multiple PV units with three different configurations. These three configurations include: (i) the direct connection of multiple PV units to the grid; (ii) the connection of multiple PV units to the grid through a point of common coupling (PCC); (iii) multiple PV units connected to the grid without a PCC but with connecting lines through all PV units are coupled with each other. The dynamic interactions are theoretically analyzed based on the generalized dynamical models. Simulation studies are carried out on an IEEE 15-bus test system to demonstrate the dynamical interactions among different PV units.

The rest of the paper is organized as follows. Section 2 includes the detailed dynamical models of grid-connected PV systems for different configurations. The dynamic interactions among different PV units are theoretically analyzed in Section 3 and simulation results are presented in Section 4 to support the analysis in terms of the power quality. Finally, the paper is concluded in Section 5 along with some future research directions.

2. Dynamical Modeling of a Grid-Connected System with Multiple PV Units

A grid-connected PV system usually comprises a PV array along with the maximum power point tracking (MPPT) system where this tracker is used to track maximum power under changing atmospheric conditions. Since the output power of the PV array is small, a DC-DC boost converter is used to achieve the desired voltage across the DC-link capacitor which is also the input voltage to the voltage source inverter (VSI). In this work, it is considered that the maximum power is extracted from the PV unit through the MPPT and the desired voltage is achieved across the DC-link capacitor. For this reason, the dynamics of the DC-DC converter is not considered during the modeling and another reason for such a consideration is that this work mainly stresses on the current injection into the grid with the power quality. Therefore, the model is basically developed based on the dynamics of the DC-link voltage and current injecting into the grid. The following subsections include the dynamical models of multiple PV units in a grid-connected PV system by considering all possible configurations.

2.1. Dynamical Modeling of a Single PV Unit Connected to the Grid

The dynamical model is first developed for a three-phase grid-connected system with a single PV unit. Figure 1 shows a grid-connected system with a single PV unit where a VSI is used as an interface. In Figure 1, the voltage across the DC-link capacitor (C) is v_{dc} while the filter resistance and inductance are represented by R_f and L_f, respectively. A transformer with an inductance L_T along with the transmission line having resistance R_L and inductance L_L is used to deliver power into the grid. By considering the output-side of the VSI, the dynamics of the currents for the three-phase grid-connected PV system in Figure 1 can be written as follows [28,29]:

$$\dot{i}_a = -\frac{R}{L}i_a - \frac{1}{L}e_a + \frac{v_{dc}}{3L}(2K_a - K_b - K_c)$$
$$\dot{i}_b = -\frac{R}{L}i_b - \frac{1}{L}e_b + \frac{v_{dc}}{3L}(-K_a + 2K_b - K_c) \qquad (1)$$
$$\dot{i}_c = -\frac{R}{L}i_c - \frac{1}{L}e_c + \frac{v_{dc}}{3L}(-K_a - K_b + 2K_c)$$

where $R = R_f + R_L$, $L = L_f + L_T + L_L$, i_{abc} represents three currents following through three phases, e_{abc} represents three voltages for three phases at the grid connection point, and K_{abc} represents three switching signals for the three-phase VSI.
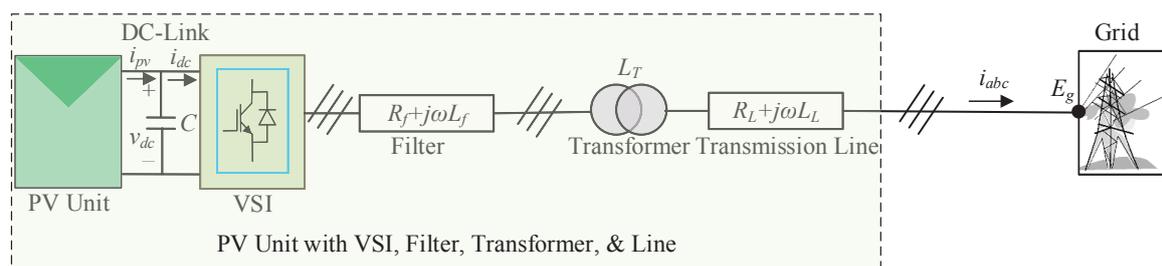

Figure 1. A single photovoltaic (PV) unit connected to the grid.

By considering the input-side of the VSI, the dynamic of the DC-link voltage can be written as follows:

$$\dot{v}_{dc} = \frac{1}{C}i_{pv} - \frac{1}{C}(i_a K_a + i_b K_b + i_c K_c) \qquad (2)$$

where i_{pv} is the output current of the PV unit.

By employing *dq* transformation, the complete dynamical model of a grid-connected PV system with a single PV unit can be written as follows [30]:

$$\dot{I}_d = -\frac{R}{L}I_d + \omega I_q - \frac{E_d}{L} + \frac{v_{dc}}{L}K_d$$

$$\dot{I}_q = -\omega I_d - \frac{R}{L}I_q - \frac{E_q}{L} + \frac{v_{dc}}{L}K_q \qquad (3)$$

$$\dot{v}_{dc} = \frac{1}{C}i_{pv} - \frac{1}{C}I_dK_d - \frac{1}{C}I_qK_q$$

The dynamical model as represented by Equation (3) can be considered as the basis for developing the same for grid-connected PV systems with multiple PV units. The dynamical model for grid-connected systems with multiple PV units are developed in the following subsection where all PV units are directly connected to the grid.

2.2. Dynamical Modeling of a Grid-Connected System with Directly Connected Multiple PV Units

Figure 2 shows a grid-connected system with multiple PV units where all PV units are directly connected to the grid through the VSI, filter, transformer and transmission/distribution line. The dynamical model of the system in Figure 2 will be exactly similar to that of the grid-connected system with a single PV unit. Thus, the dynamical model of *i*th PV unit can be written as follows:

$$\dot{I}_{di} = -\frac{R_i}{L_i}I_{di} + \omega I_{qi} - \frac{E_d}{L_i} + \frac{v_{dci}}{L_i}K_{di}$$

$$\dot{I}_{qi} = -\omega I_{di} - \frac{R_i}{L_i}I_{qi} - \frac{E_q}{L_i} + \frac{v_{dci}}{L_i}K_{qi} \qquad (4)$$

$$\dot{v}_{dci} = \frac{1}{C_i}i_{pvi} - \frac{1}{C_i}I_{di}K_{di} - \frac{1}{C_i}I_{qi}K_{qi}$$

with $R_i = R_{fi} + R_{Li}$ and $L_i = L_{fi} + L_{Ti} + L_{Li}$ with i = 1, 2, 3, $\cdots$, n.
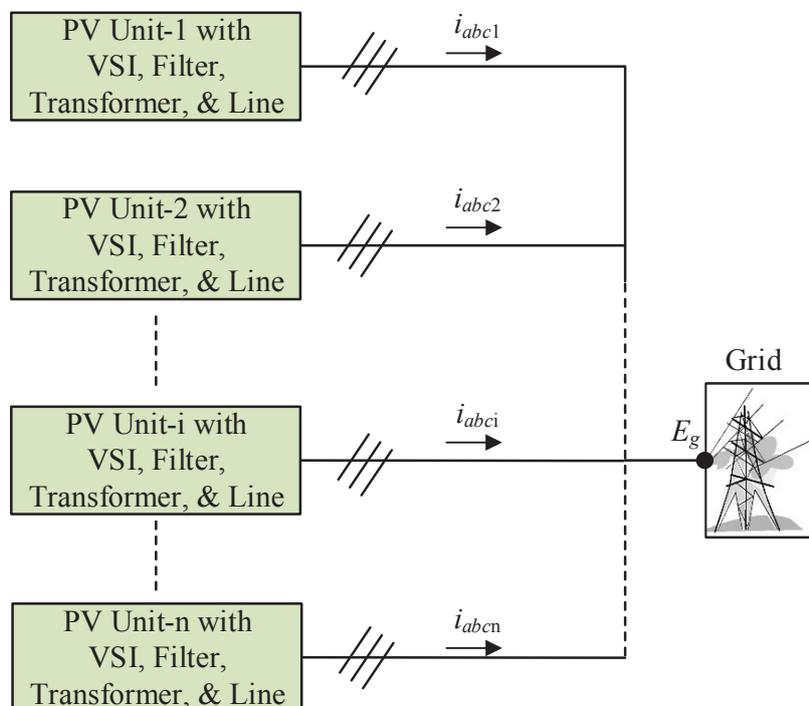

Figure 2. Multiple PV units directly connected to the grid.

2.3. Dynamical Modeling of a Grid-Connected System with Multiple PV Units Connected through a PCC

Figure 3 shows another configuration for the grid-connected system with multiple PV units where all PV units are first connected to a PCC through the VSI, filter, transformer and transmission/distribution line. The PCC is then connected to the grid via a transmission/distribution line with the resistance R_{Lg} and inductance L_{Lg}. In this case, the dynamical model will be different from previous cases. The current for ith PV unit flowing through different phases can be written as follows:

$$
\begin{aligned}
\dot{i}_{ai} &= -\frac{R'}{L'}i_{ai} - \frac{1}{L'}e_a + \frac{v_{dci}}{3L'}K_{abc1} - \frac{1}{L'}\sum_{\substack{k=1\\k\neq i}}^{n} v_{gak} \\
\dot{i}_{bi} &= -\frac{R'}{L'}i_{bi} - \frac{1}{L'}e_b + \frac{v_{dci}}{3L'}K_{abc2} - \frac{1}{L'}\sum_{\substack{k=1\\k\neq i}}^{n} v_{gbk} \\
\dot{i}_{ci} &= -\frac{R'}{L'}i_{ci} - \frac{1}{L'}e_c + \frac{v_{dci}}{3L'}K_{abc3} - \frac{1}{L'}\sum_{\substack{k=1\\k\neq i}}^{n} v_{gck}
\end{aligned}
\tag{5}
$$

where $R' = R_i + R_{Lg}$, $L' = L_i + L_{Lg}$, $K_{abc1} = 2K_{ai} - K_{bi} - K_{ci}$, $K_{abc2} = -K_{ai} + 2K_{bi} - K_{ci}$, $K_{abc3} = -K_{ai} - K_{bi} + 2K_{ci}$, $v_{gk} = v_{Lgk} + v_{Rgk} = L_{Lg}\frac{di_k}{dt} + R_{Lg}i_k$ for all three phases. The last terms in Equation (5), i.e., $\sum_{\substack{k=1\\k\neq i}}^{n} v_{gak}$, $\sum_{\substack{k=1\\k\neq i}}^{n} v_{gbk}$, and $\sum_{\substack{k=1\\k\neq i}}^{n} v_{gck}$ represent the dynamic interactions which have sinusoidal characteristics. However, these terms are converted into *dq*-frame later in this subsection to further simplify the analysis. The dynamic of the DC-link voltage will remain similar to that of the previous case.
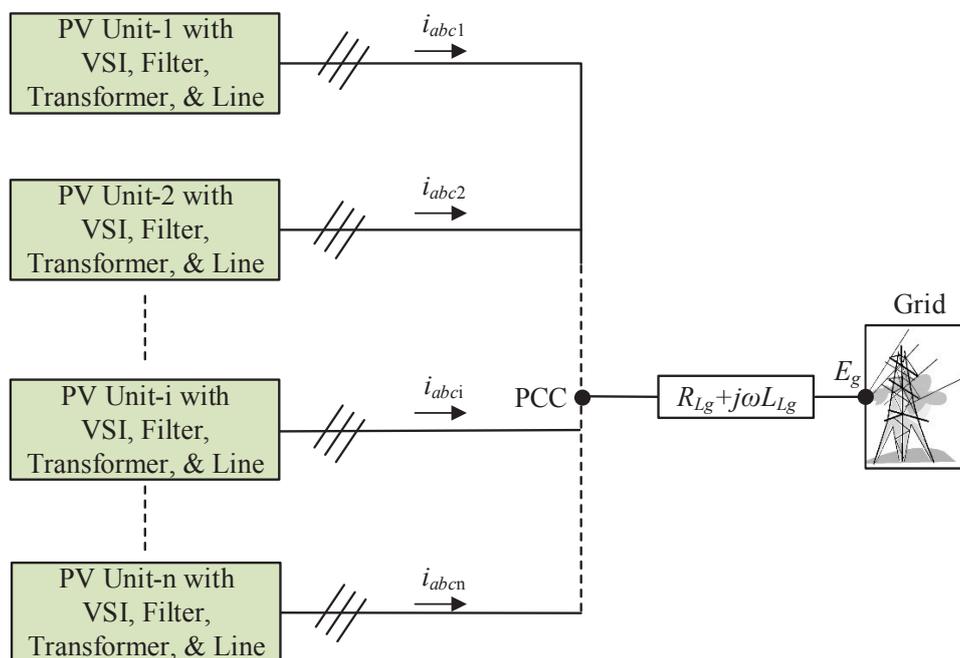

Figure 3. Multiple PV units connected to the grid through a point of common coupling (PCC).

In *dq*–frame, Equation (5) along with the dynamic of the DC-link voltage can be written as follows:

$$\dot{I}_{di} = -\frac{R'}{L'}I_{di} + \omega I_{qi} - \frac{E_d}{L'} + \frac{v_{dci}}{L'}K_{di} - \frac{1}{L'}\sum_{\substack{k=1 \\ k \neq i}}^{n} V_{gdk}$$

$$\dot{I}_{qi} = -\frac{R'}{L'}I_{qi} - \omega I_{di} - \frac{E_q}{L'} + \frac{v_{dci}}{L'}K_{qi} - \frac{1}{L'}\sum_{\substack{k=1 \\ k \neq i}}^{n} V_{gqk} \qquad (6)$$

$$\dot{v}_{dci} = \frac{1}{C_i}i_{pvi} - \frac{1}{C_i}I_{di}K_{di} - \frac{1}{C_i}I_{qi}K_{qi}$$

2.4. Dynamical Modeling of a Grid-Connected System with Multiple PV Units Interconnected through Lines

Figure 4 shows the interconnection of multiple PV units through different lines rather than connected through a PCC. In this configuration, all PV units are strongly coupled through lines with resistance R_{Lij} and inductance L_{Lij} between bus-i and bus-j. From Figure 4, the current for ith PV unit flowing through different phases can be written as follows:

$$i_{ai} = -\frac{R'_{\Sigma}}{L'_{\Sigma}}i_{ai} - \frac{1}{L'_{\Sigma}}e_a + \frac{v_{dci}}{3L'_{\Sigma}}K_{abc1} - \frac{1}{L'_{\Sigma}}\alpha_a$$

$$i_{bi} = -\frac{R'_{\Sigma}}{L'_{\Sigma}}i_{bi} - \frac{1}{L'_{\Sigma}}e_b + \frac{v_{dci}}{3L'_{\Sigma}}K_{abc2} - \frac{1}{L'_{\Sigma}}\alpha_b \qquad (7)$$

$$i_{ci} = -\frac{R'_{\Sigma}}{L'_{\Sigma}}i_{ci} - \frac{1}{L'_{\Sigma}}e_c + \frac{v_{dci}}{3L'_{\Sigma}}K_{abc1} - \frac{1}{L'_{\Sigma}}\alpha_c$$

where $R'_{\Sigma} = R_i + R_{Lg} + \sum_{\substack{j=1 \\ j \neq i}}^{n} \beta_j\gamma_{ij}R_{Lij}$, $L'_{\Sigma} = L_i + L_{Lg} + \sum_{\substack{j=1 \\ j \neq i}}^{n} \beta_j\gamma_{ij}L_{Lij}$, $\alpha = \left(\sum_{\substack{k=1 \\ k \neq i}}^{n} v_{gk} + \sum_{\substack{j=1 \\ j \neq i}}^{n} v_{cj}\right)$ for all three phases, $v_{cj} = \beta_j(v_{Lcj} + v_{Rcj}) = \beta_j\left(L_{Lij}\frac{di_j}{dt} + R_{Lij}i_j\right)$ for all three phases, β_j is a flow function which represents the existence of current flow through the interconnecting line due to other PV unit, and γ_{ij} represents the interconnection between different PV units. The value of β_j will be zero when there are no current flow and it will be one if there exists current flow. Similarly, the value of γ_{ij} will be zero if there are no interconnections while it is one if there are interconnections.
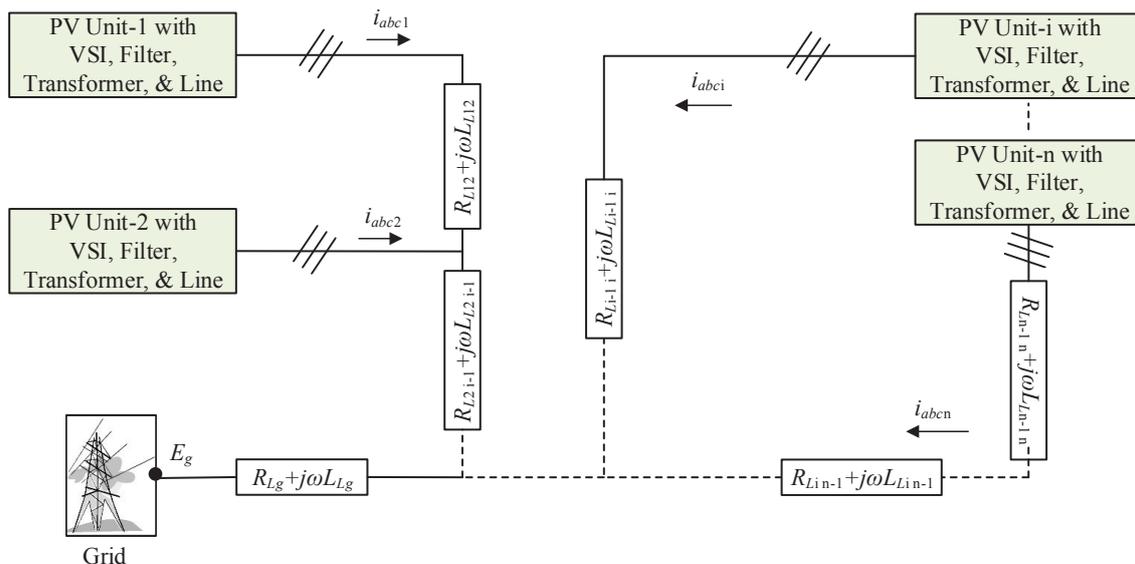

Figure 4. Multiple PV units connected to the grid through a lines.

The dynamic of the DC-link voltage will remain similar to that of all previous cases. In dq–frame, Equation (7) along with the dynamic of the DC-link voltage can be written as follows:

$$
\begin{aligned}
\dot{I}_{di} &= -\frac{R'_{\Sigma}}{L'_{\Sigma}}I_{di} + \omega I_{qi} - \frac{E_d}{L'_{\Sigma}} + \frac{v_{dci}}{L'_{\Sigma}}K_{di} - \frac{1}{L'_{\Sigma}}\alpha_d \\
\dot{I}_{qi} &= -\frac{R'_{\Sigma}}{L'_{\Sigma}}I_{qi} - \omega I_{di} - \frac{E_q}{L'_{\Sigma}} + \frac{v_{dci}}{L'_{\Sigma}}K_{qi} - \frac{1}{L'_{\Sigma}}\alpha_q \\
\dot{v}_{dci} &= \frac{1}{C_i}i_{pvi} - \frac{1}{C_i}I_{di}K_{di} - \frac{1}{C_i}I_{qi}K_{qi}
\end{aligned}
\tag{8}
$$

where

$$
\alpha_d = \left(\sum_{\substack{k=1 \\ k \neq i}}^{n} V_{gdk} + \sum_{\substack{j=1 \\ j \neq i}}^{n} V_{cdj} \right) \text{ and } \alpha_q = \left(\sum_{\substack{k=1 \\ k \neq i}}^{n} V_{gqk} + \sum_{\substack{j=1 \\ j \neq i}}^{n} V_{cqj} \right)
$$

Equations (4), (6), and (8) represent the generalized dynamical models for three different configurations. The following section includes a theoretical analysis of dynamic interactions based on these dynamical models.

3. Analysis of Dynamic Interactions

From the dynamical models of multiple PV units in the first configuration as shown in Figure 2, it can be seen from Equation (4) that there are no direct interactions among different PV units. However, there will still be some dynamical interactions which are mainly through the grid connection points. In this case, the output current of each PV unit will contain some harmonics and the THD will be increased with an increase in the number of PV units.

For the second configuration in Figure 3, there are dynamic interactions which can be seen from Equation (6). These interactions are mainly due to the voltage drop for flowing current in the line from other PV units where the line connects the PCC with the grid. In this case, the THD will be slightly less than the first configuration as the output current of each PV unit flow through an additional inductance which is also obvious from the term L' in Equation (6).

The configuration in Figure 4 is quite complicated and thus, the dynamical model as represented by Equation (8) is also more complicated. In this model, the interactions mainly depend on the flow of the current as well the the coupling between lines. The dynamic interactions among different PV units in Figure 4 are more than all other configurations due to additional lines which establish connections among all PV units within the grid-connected system. This phenomenon is also obvious from Equation (8) from where it can be seen that it includes more additional terms than any other configurations. However, the THD will be less in this case because the value of inductance (L'_{Σ}) through which the current flows is much higher than all other configurations. Simulation results are carried out in the following section to further justify these analyses.

4. Simulation Results

The dynamic interactions among different PV units are analyzed by carrying out simulations on an IEEE 15-bus test system as shown in Figure 5. The detailed parameters of the connecting lines are provided in Table 1. Multiple PV units are connected at bus-3 by considering three different configurations. In this section, the configurations in Figures 2–4 are considered as configurations *a*, *b*, and *c* (CONF-*a*, CONF-*b*, and CONF-*c*), respectively. For all these configurations, three PV units (PV-1, PV-2, and PV-3) are considered to analyze the dynamic interactions, i.e., $n = 3$. The maximum power capacities of PV-1, PV-2, and PV-3 are considered as 6.1 kW, 9.5 kW, and 3.29 kW, respectively. The interactions are analyzed in terms of THD in the current of a PV unit and in this

simulation, the second PV unit (PV-2) is considered as the reference unit. According to IEEE standard, the acceptable THD in the output current of a VSI is 5 percent.

Table 1. Line Parameters.

Parameter	Value
R_{f1}	0.16 mΩ
L_{f1}	34.25 μH
R_{f2}	0.22 mΩ
L_{f2}	34.25 μH
R_{f3}	0.21 mΩ
L_{f3}	34 μH
R_{Li}	1.53 Ω
L_{Li}	3 mH
$R_{Lij}(i \neq j)$	1.35 Ω
$L_{Lij}(i \neq j)$	2.1 mH
R_{Ti}	0.06 Ω
L_{Ti}	0.53 mH
R_{Lgi}	0.12 Ω
L_{Lgi}	1.05 mH
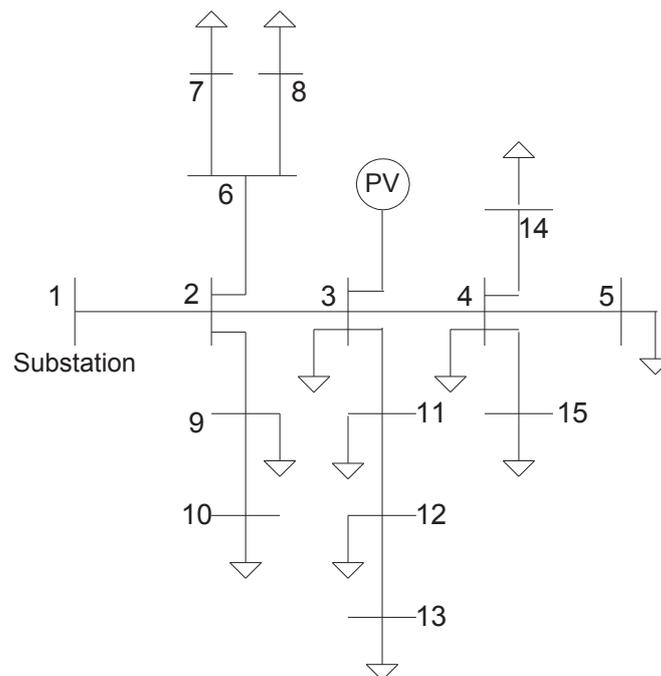
Figure 5. IEEE 15-bus test system with multiple PV units at bus-3.

At the beginning of the simulation, the output current of the PV-2 is observed for CONF-*a* solely with this PV unit. From Figure 6, it can be seen that the current of PV-2 is sinusoidal with $n = 1$ though the current responses are distorted with the increases in PV units. It is worth to note that only a certain portion of the waveform is considered to clearly present the distortions in the waveform. The corresponding THDs are shown in Figure 7 from where it can be clearly seen that the values of THDs increase with the increase in PV units within the system. Initially, the THD in the current of the PV-2 is 0.14 percent and it increases to 0.9 percent when another PV unit is connected while it becomes 2.94 percent when all three PV units are connected. The THDs for all other PV units are also observed at the same time and it is observed that the THD in the output current of the PV-1 is

8.70 percent when all PV units are connected though its initial value was 0.14 percent. Therefore, it can be said that the values of THDs become undesirable for some PV units in a grid-connected system. However, the values of THD will be far away from the acceptable limit when more PV units are connected with the grid.
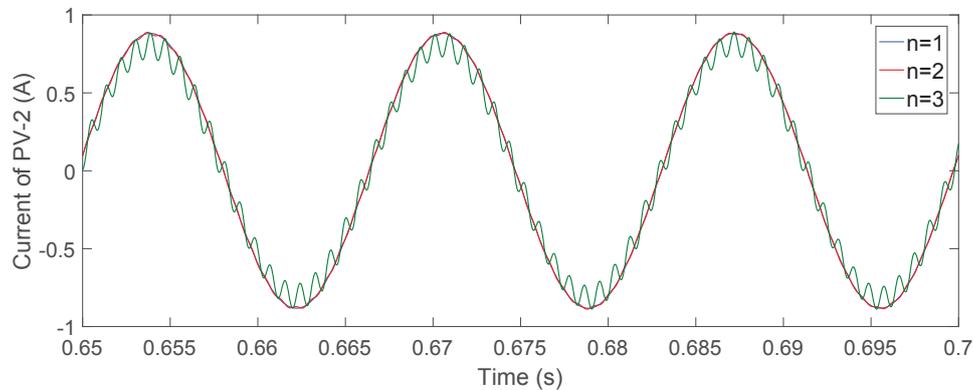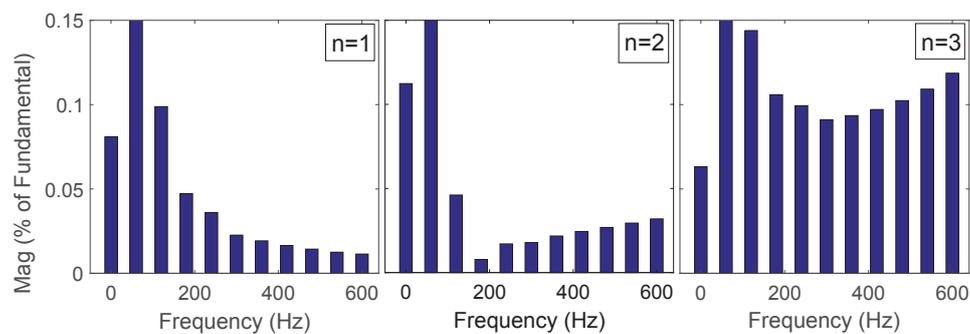

Figure 6. Output current of PV-2 for CONF-*a*.

Figure 7. Total harmonic distortions (THD) in the output current of PV-2 CONF-*a*.

A similar operating condition is considered for CONF-*b* for which the current response of the PV-2 is shown in Figure 8 where the current responses exhibit quite similar characteristics to that of CONF-*a*, i.e., these responses are distorted with the increase in the number of PV units. The THDs corresponding to these currents are shown in Figure 9. For this configuration, the value of THD is slightly lower (0.84 percent) when one more PV unit is connected, i.e., $n = 2$ though it is 0.14 percent for $n = 1$. However, it increases from 0.84 percent to 2.81 percent for $n = 3$. In this situation, the THD in the output current of the PV-1 is 8.27 percent which is still more than 5 percent. Therefore, the dynamic interactions among multiple PV units for CONF-*b* also deteriorates the power quality of other PV units within the system.

The dynamic interactions among multiple PV units are finally analyzed for CONF-*c* and in this case, the system is first simulated with at least two PV units rather than a single PV unit as considered for previous two configurations. The current responses still show the similar behaviors, i.e., these responses are distorted when the number of PV units increases which can also be seen from Figure 10. The THDs in Figure 11 clearly show that these values are lower than two other configurations. When $n = 2$, the value of the THD in the output current of the PV-2 is 0.71 percent and it is 2.32 percent when all three PV units are connected to the system through lines. However, the THD in the output current for the PV-1 is 6.73 percent which exceeds the acceptable limits.

Simulation results for all configurations clearly show that there exist dynamic interactions with increases in PV units. In all cases, the dynamics of one PV unit deteriorate the power quality of other PV units within the system.
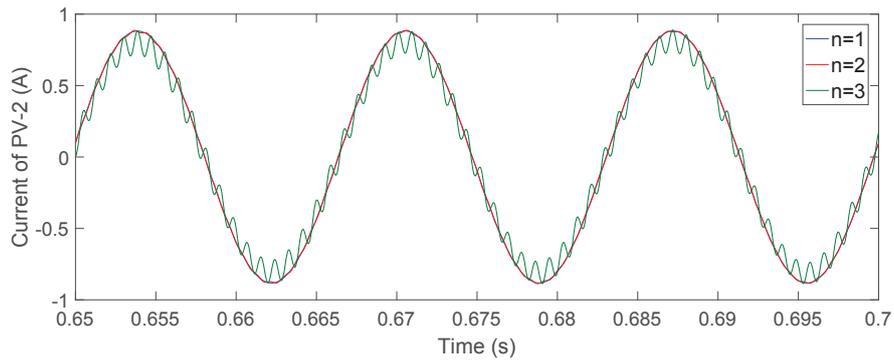
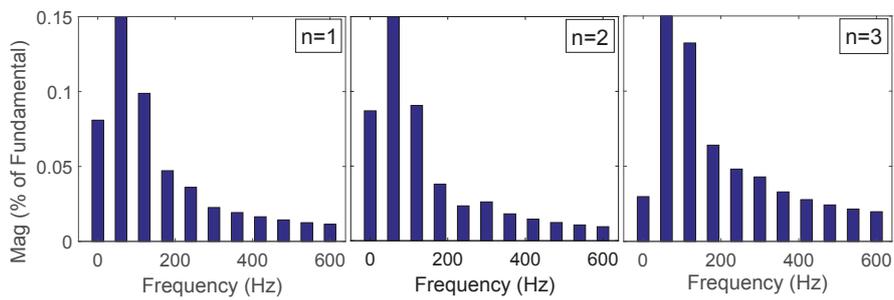**Figure 8.** Output current of PV-2 for CONF-*b*.
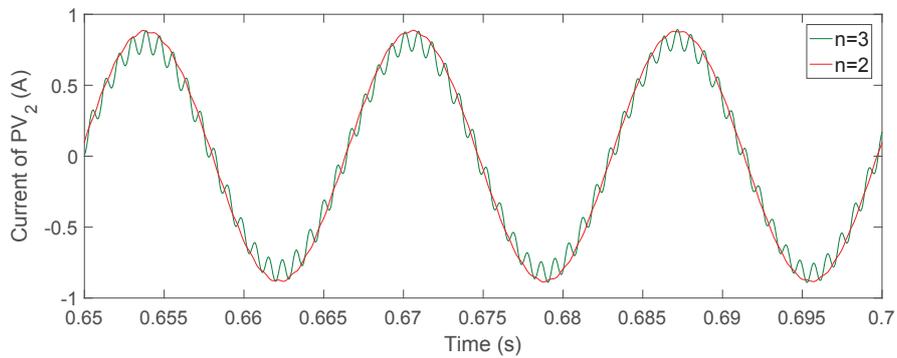

Figure 9. THD in the output current of PV-2 CONF-*b*.

Figure 10. Output current of PV-2 for CONF-*c*.
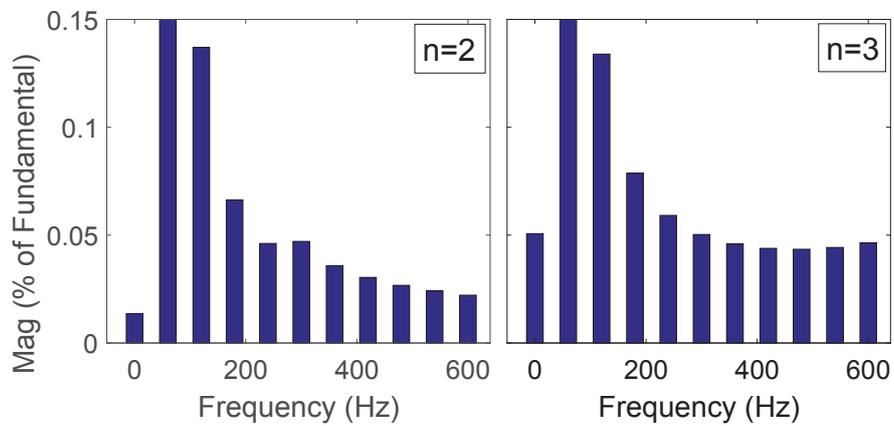

Figure 11. THD in the output current of PV-2 CONF-*c*.

5. Conclusions

The dynamic interactions among multiple PV units along with their interconnections to the main grid are analyzed. The comprehensive and generalized dynamical models are developed for multiple PV units in grid-connected PV systems by considering all possible configurations. The dynamic interactions among multiple PV units are first theoretically analyzed by representing these in terms of voltage drops and impedances of connecting lines. The developed models also have demonstrated that the direction of currents are important for analyzing dynamic interactions among PV units when these are connected with each other via lines. From these developed models, it is found that the PV systems are correlated with each other by coefficients where these coefficients are represented by resistive and inductive elements of the lines. If there are no interconnections among several PV units, the terms related to dynamic interactions become zero though these interactions increase if PV units are placed in close proximities. Moreover, a general trend is found for the degradation of power quality with increases in the number of PV units. Simulation results on an IEEE 15-bus test system clearly demonstrate the matching of the theoretical phenomena which are analyzed through the developed dynamical models. The developed dynamical models and the outcomes from dynamic interactions can be used in future research to design controllers for eliminating these interactions among multiple PV units as well as to improve the power quality.

References

1. Korkas, C.D.; Baldi, S.; Michailidis, I.; Kosmatopoulos, E.B. Occupancy-based demand response and thermal comfort optimization in microgrids with renewable energy sources and energy storage. *Appl. Energy* **2016**, *163*, 93–104.
2. Baldi, S.; Karagevrekis, A.; Michailidis, I.T.; Kosmatopoulos, E.B. Joint energy demand and thermal comfort optimization in photovoltaic-equipped interconnected microgrids. *Energy Convers. Manag.* **2015**, *101*, 352–363.
3. Navarro, A.A.; Ramírez, L.; Domínguez, P.; Blanco, M.; Polo, J.; Zarza, E. Review and validation of Solar Thermal Electricity potential methodologies. *Energy Convers. Manag.* **2016**, *126*, 42–50.
4. Marzband, M.; Yousefnejad, E.; Sumper, A.; Dominguez-Garcia, J.L. Real time experimental implementation of optimum energy management system in standalone Microgrid by using multi-layer ant colony optimization. *Int. J. Electr. Power Energy Syst.* **2016**, *75*, 265–274.
5. Marzband, M.; Ghadimi, M.; Sumper, A.; Dominguez-Garcia, J.L. Experimental validation of a real-time energy management system using multi-period gravitational search algorithm for microgrids in islanded mode. *Appl. Energy* **2014**, *128*, 164–174.
6. Australian Energy Market Operator. *National Electricity Forecasting Report for the National Electricity Market*; Technical Report; Australian Energy Market Operator (AEMO): Melbourne, Australia, 2016.
7. Hossain, E.; Kabalci, E.; Bayindir, R.; Perez, R. Microgrid testbeds around the world: State of art. *Energy Convers. Manag.* **2014**, *86*, 132–153.
8. Hossain, M.J.; Saha, T.K.; Mithulananthan, N.; Pota, H.R.; Lu, J. Dynamic interactions among multiple DER controllers in distribution systems. In Proceedings of the 2012 IEEE International Conference on Power System Technology (POWERCON), Auckland, New Zealand, 30 October–2 November 2012; pp. 1–6.
9. Enslin, J.H.R.; Heskes, P.J.M. Harmonic interaction between a large number of distributed power inverters and the distribution network. *IEEE Trans. Power Electron.* **2004**, *19*, 1586–1593.
10. Infield, D.G.; Onions, P.; Simmons, A.D.; Smith, G.A. Power quality from multiple grid-connected single-phase inverters. *IEEE Trans. Power Deliv.* **2004**, *19*, 1983–1989.
11. Tan, Y.T.; Kirschen, D.S.; Jenkins, N. A model of PV generation suitable for stability analysis. *IEEE Trans. Energy Convers.* **2004**, *19*, 748–755.

12. Kouro, S.; Leon, J.I.; Vinnikov, D.; Franquelo, L.G. Grid-Connected Photovoltaic Systems: An Overview of Recent Research and Emerging PV Converter Technology. *IEEE Ind. Electron. Mag.* **2015**, *9*, 47–61.

13. Tan, Y.T.; Kirschen, D.S. Impact on the Power System of a Large Penetration of Photovoltaic Generation. In Proceedings of the 2007 IEEE Power Engineering Society General Meeting, Tampa, FL, USA, 24–28 June 2007; pp. 1–8.

14. Perera, B.K.; Pulikanti, S.R.; Ciufo, P.; Perera, S. Simulation model of a grid-connected single-phase photovoltaic system in PSCAD/EMTDC. In Proceedings of the 2012 IEEE International Conference on Power System Technology (POWERCON), Auckland, New Zealand, 30 October–2 November 2012; pp. 1–6.

15. Refaat, S.S.; Abu-Rub, H.; Sanfilippo, A.P.; Mohamed, A. Impact of grid-tied large-scale photovoltaic system on dynamic voltage stability of electric power grids. *IET Renew. Power Gener.* **2017**, doi:10.1049/iet-rpg.2017.0219.

16. Kim, S.K.; Jeon, J.H.; Cho, C.H.; Kim, E.S.; Ahn, J.B. Modeling and simulation of a grid-connected PV generation system for electromagnetic transient analysis. *Solar Energy* **2009**, *83*, 664–678.

17. Xiao, W.; Edwin, F.F.; Spagnuolo, G.; Jatskevich, J. Efficient Approaches for Modeling and Simulating Photovoltaic Power Systems. *IEEE J. Photovolt.* **2013**, *3*, 500–508.

18. Yazdani, A.; Fazio, A.R.D.; Ghoddami, H.; Russo, M.; Kazerani, M.; Jatskevich, J.; Strunz, K.; Leva, S.; Martinez, J.A. Modeling Guidelines and a Benchmark for Power System Simulation Studies of Three-Phase Single-Stage Photovoltaic Systems. *IEEE Trans. Power Deliv.* **2011**, *26*, 1247–1264.

19. Baimel, D.; Belikov, J.; Guerrero, J.M.; Levron, Y. Dynamic Modeling of Networks, Microgrids, and Renewable Sources in the dq0 Reference Frame: A Survey. *IEEE Access* **2017**, *5*, 21323–21335.

20. Shah, R.; Mithulananthan, N.; Bansal, R.C. Oscillatory stability analysis with high penetrations of large-scale photovoltaic generation. *Energy Convers. Manag.* **2013**, *65*, 420–429.

21. Liu, J.; Zhou, L.; Li, B.; Zheng, C.; Xie, B. Modeling and Analysis of a Digitally Controlled Grid-Connected Large-Scale Centralized PV System. *IEEE Trans. Power Electron.* **2017**, *PP*, 1, doi:10.1109/TPEL.2017.2712910.

22. Nduka, O.S.; Pal, B.C. Harmonic Domain Modeling of PV System for the Assessment of Grid Integration Impact. *IEEE Trans. Sustain. Energy* **2017**, *8*, 1154–1165.

23. Tamimi, B.; Cañizares, C.; Bhattacharya, K. System Stability Impact of Large-Scale and Distributed Solar Photovoltaic Generation: The Case of Ontario, Canada. *IEEE Trans. Sustain. Energy* **2013**, *4*, 680–688.

24. Yazdani, A.; Dash, P.P. A Control Methodology and Characterization of Dynamics for a Photovoltaic (PV) System Interfaced with a Distribution Network. *IEEE Trans. Power Deliv.* **2009**, *24*, 1538–1551.

25. Agorreta, J.L.; Borrega, M.; López, J.; Marroyo, L. Modeling and Control of *N* -Paralleled Grid-Connected Inverters with *LCL* Filter Coupled Due to Grid Impedance in PV Plants. *IEEE Trans. Power Electron.* **2011**, *26*, 770–785.

26. Akhavan, A.; Mohammadi, H.R.; Guerrero, J.M. Modeling and design of a multivariable control system for multi-paralleled grid-connected inverters with *LCL* filter. *Int. J. Electr. Power Energy Syst.* **2018**, *94*, 354–362.

27. Zhao, Z.; Yang, P.; Wang, Y.; Xu, Z.; Guerrero, J.M. Dynamic Characteristics Analysis and Stabilization of PV-Based Multiple Microgrid Clusters. *IEEE Trans. Smart Grid* **2017**, *PP*, doi:10.1109/TSG.2017.2752640.

28. Lalili, D.; Mellit, A.; Lourci, N.; Medjahed, B.; Berkouk, E.M. Input output feedback linearization control and variable step size MPPT algorithm of a grid-connected photovoltaic inverter. *Renew. Enegry* **2011**, *36*, 3282–3291.

29. Marouani, R.; Mami, A. Robust maximum power point tracker using sliding mode controller for the three-phase grid-connected photovoltaic system. *Am. J. Appl. Energy* **2010**, *7*, 1168–1173.

30. Mahmud, M.A.; Pota, H.R.; Hossain, M.J. Dynamic Stability of Three-Phase Grid-Connected Photovoltaic System Using Zero Dynamic Design Approach. *IEEE J. Photovolt.* **2012**, *2*, 564–571.